Diagnostic BioSystems

Instructions For Use

KT 034-IFU

Document #: DS-3026-C	Release Date: 07/02/2024

6616 Owens Drive, Pleasanton, CA 94588 U.S.A. - Tel. (925) 484-3350 - Fax (925) 484-3390 - www.dbiosys.com

Trichrome Stain Kit

(Modified Masson's)

Description and Principle

The Trichrome Stain Kit (Modified Masson's) is intended for use in the histological visualization of collagenous connective tissue fibers in tissue sections. This kit may be used on formalin-fixed, paraffin-embedded sections.

This kit utilizes 3 dye solutions used in sequence along with an Iron hematoxylin solution that resists decolorization by subsequent acidic stain solutions. Sections are first mordanted in heated Bouin's Fluid which acts to intensify the subsequent trichrome stains. Biebrich Scarlet / Acid Fuchsin Solution stains all acidophilic tissue elements red. Phosphomolybdic and phosphotungstic acids displace the red dye out of collagen fibers leaving them colorless and receptive to staining by aniline blue.

Expected Results

Collagen:	Blue
Muscle Fibers:	Red
Nuclei:	Dark Red to Black/Blue

Kit Contents	Storage
1. Bouin's Fluid	15-30°C
2. Weigert's Iron, Hematoxylin (A)	15-30°C
3. Weigert's Iron, Hematoxylin (B)	15-30°C
4. Biebrich Scarlet / Acid Fuchsin Solution	15-30°C
5. Phosphomolybdic/Phosphotungstic Acid Solution	15-30°C
6. Aniline Blue Solution	15-30°C
7. Acetic Acid Solution (1%)	15-30°C

Suggested Controls *(not provided)*

Lung, Liver, Colon, Stomach.

Uses/Limitations

For In-Vitro Diagnostic use only.
Do not use if reagents become cloudy or precipitate
Do not use past expiration date.
Use caution when handling reagents.
Non-Sterile
Intended for FFPE sections cut at 5-10µm.
This procedure has not been optimized for frozen sections.
Frozen sections may require protocol modification.

Storage

Store kit and all components at room temperature (15-30°C).

Safety and Precautions

Please see current Safety Data Sheets (SDS) for this product and components GHS classification, pictograms, and full hazard/precautionary statements. If there is any serious incident that has occurred in relation to the device, please contact the manufacturer: Diagnostic BioSystems Technical Support at (925) 484-3350, extension 2 or techsupport@dbiosys.com. If required, please report to the Competent Authority of the Member State in which the user and/or patient is established.

Important Notes:

1. If final background is dark or dull red/blue, it may be caused by excess gray background from Weigert's Iron Hematoxylin. If this is the case, reduce staining time of Weigert's Iron Hematoxylin for future slides (step 6). A standard Acid Alcohol solution (not provided) may also be used to remove excess gray background immediately after step 6 as well.

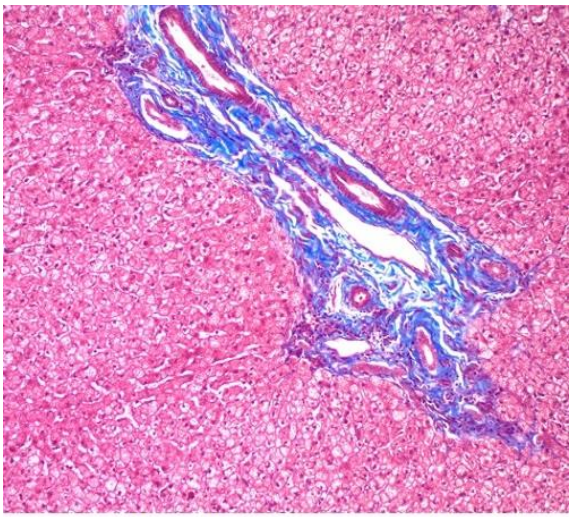

Human Liver stained with Trichrome Stain Kit (Modified Masson's) viewed at 100X magnification

2. Differentiating strength of Phosphomolybdic/Phosphotungstic Acid Solution is greatly increased by mixing **1:1** with ethanol (not provided). This modification may allow better visualization of small collagen fibers than the traditional method, but will remove red stain much more quickly so should be done with caution:

For example, mix:

-1ml of ethanol
-1ml of Phosphomolybdic/ Phosphotungstic Acid Solution

*Replace step 11 by applying **1:1** working solution to tissue for **2-6** minutes. Check slide microscopically for proper differentiation and repeat if needed. Rinse well with deionized water after differentiation.*

Procedure:

1. Deparaffinize sections if necessary and hydrate to distilled water.

2. Preheat Bouin's Fluid in a water bath to 56° - 64° centigrade in a fume hood or very well-ventilated area.

3. Place slides in preheated Bouin's Fluid for 60 minutes followed by a 10-minute cooling period.

4. Rinse slide in tap water until section is completely clear.

5. Rinse once in distilled water.

6. Mix equal parts of Weigert's (A) and Weigert's (B) and stain slide with working Weigert's Iron Hematoxylin for 2-4 minutes. Stain is alcoholic and

Diagnostic BioSystems
6616 Owens Drive
Pleasanton, CA, 94588
Tel: (925) 484 3350
www.dbiosys.com

CH REP
MedEnvoy Switzerland
Gotthardstrasse 28
6302 Zug
Switzerland

EC REP
MedEnvoy Global B.V.
Prinses Margrietplantsoen 33 - Suite 123
2595 AM The Hague
The Netherlands

IVD

prone to evaporation – monitor and add stain as necessary to ensure stain does not dry on slide. Dried stain may result in excess grey background.

7. Rinse slide in running tap water for 2 minutes.

8. Rinse slide in distilled water.

9. Apply Biebrich Scarlet / Acid Fuchsin Solution to slide for 5-10 minutes.

10. Rinse slide in distilled water.

11. Differentiate in Phosphomolybdic/Phosphotungstic Acid Solution for 10-15 minutes. *Note: See alternative modification in Important Note #2 above.*

12. Without rinsing, apply Aniline Blue Solution to slide for 5-10 minutes.

13. Rinse slide in distilled water.

14. Apply Acetic Acid Solution (1%) to slide for 3-5 minutes.

15. Dehydrate very quickly in 2 changes of 95% Alcohol, followed by 2 changes of Absolute Alcohol.

16. Clear in Xylene or Xylene Substitute, and mount in synthetic resin.

References

1. Liu, CT., Hsu, SC., Hsieh, HL. et al. Inhibition of β-catenin signaling attenuates arteriovenous fistula thickening in mice by suppressing myofibroblasts. Mol Med 28, 7 (2022). https://doi.org/10.1186/s10020-022-00436-1
2. Zwaans, B.M.M., Carabulea, A.L., Bartolone, S.N. et al. Voiding defects in acute radiation cystitis driven by urothelial barrier defect through loss of E-cadherin, ZO-1 and Uroplakin III. Sci Rep 11, 19277 (2021). https://doi.org/10.1038/s41598-021-98303-2
3. Kao CT, Chiu YC, Lee AK, Lin YH, Huang TH, Liu YC, Shie MY. The synergistic effects of Xu Duan combined Sr-contained calcium silicate/poly-ε-caprolactone scaffolds for the promotion of osteogenesis marker expression and the induction of bone regeneration in osteoporosis. Materials Science and Engineering: C. 2021 Feb;119:111629.
4. Zwaans BM, Wegner KA, Bartolone SN, Vezina CM, Chancellor MB, Lamb LE. Radiation cystitis modeling: A comparative study of bladder fibrosis radio-sensitivity in C57BL/6, C3H, and BALB/c mice. Physiological reports. 2020 Feb;8(4):e14377.
5. Lin YY, Hong Y, Yu SH, Wu XB, Shyu WC, chen JS, Ting H, Yang AL, Lee SD. Anti-apoptotic and Mitochondrial Biogenetic Effects of Exercise Training on Ovariectomized Hypertensive Rat Hearts. Journal of Applied Physiology. 2019 Apr 18.
6. Callaghan NI, Capaz JC, Lamarre SG, Bourloutski E, Oliveira AR, MacCormack TJ, Driedzic WR, Sykes AV. Reversion to developmental pathways underlies rapid arm regeneration in juvenile European cuttlefish, Sepia officinalis (Linnaeus 1758). Journal of Experimental Zoology Part B: Molecular and Developmental Evolution. 2019 Mar 19.
7. Chang RL, Nithiyanantham S, Kuo WW, Pai PY, Chang TT, Lai CH, Chen RJ, Vijaya Padma V, Huang CY, Huang CY. Overexpression of IGF-IIRα regulates cardiac remodeling and aggravates high salt induced apoptosis and fibrosis in transgenic rats. Environmental toxicology. 2019 Feb;34(2):210-8.
8. Feng W, Lei T, Wang Y, Feng R, Yuan J, Shen X, Wu Y, Gao J, Ding W, Lu Z. GCN2 deficiency ameliorates cardiac dysfunction in diabetic mice by reducing lipotoxicity and oxidative stress. Free Radical Biology and Medicine. 2019 Jan 1;130:128-39.
9. Chang RL, Nithiyanantham S, Kuo WW, Pai PY, Chang TT, Lai CH, Chen RJ, Vijaya Padma V, Huang CY, Huang CY. Overexpression of IGF-IIRα regulates cardiac remodeling and aggravates high salt induced apoptosis and fibrosis in transgenic rats. Environmental Toxicology. 2018 Nov 18.
10. Liu S, Yuan J, Yue W, Bi Y, Shen X, Gao J, Xu X, Lu Z. GCN2 deficiency protects against high fat diet induced hepatic steatosis and insulin resistance in mice. Biochimica et Biophysica Acta (BBA)-Molecular Basis of Disease. 2018 Oct 1;1864(10):3257-67.
11. Miyazaki T, Haraguchi S, Kim-Kaneyama JR, Miyazaki A. Endothelial calpain systems orchestrate myofibroblast differentiation during wound healing. The FASEB Journal. 2018 Sep 10:fj-201800588RR.
12. Zhang Y, Feng J, Wang Q, Zhao S, Xu J, Li H. PPAR-γ agonist rosiglitazone ameliorates peritoneal deterioration in peritoneal dialysis rats with LPS-induced peritonitis through upregulation of AQP-1 and ZO-1. Bioscience reports. 2018 Jun 5:BSR20180009.
13. Yasuda Y, Iwama S, Kiyota A, Izumida H, Nakashima K, Iwata N, Ito Y, Morishita Y, Goto M, Suga H, Banno R. Critical role of rabphilin-3A in the pathophysiology of experimental lymphocytic neurohypophysitis. The Journal of pathology. 2018 Apr;244(4):469-78.
14. Feng M, Tang PM, Huang XR, Sun SF, You YK, Xiao J, Lv LL, Xu AP, Lan HY. TGF-β Mediates Renal Fibrosis via the Smad3-Erbb4-IR Long Noncoding RNA Axis. Molecular Therapy. 2018 Jan 3;26(1):148-61.
15. Lin YC, Lin YC, Kuo WW, Shen CY, Cheng YC, Lin YM, Chang RL, Padma VV, Huang CY, Huang CY. Platycodin D Reverses Pathological Cardiac Hypertrophy and Fibrosis in Spontaneously Hypertensive Rats. The American journal of Chinese medicine. 2018;46(03):537-49.
16. Kim JH, Suk S, Jang WJ, Lee CH, Kim JE, Park JK, Kweon MH, Kim JH, Lee KW. Salicornia Extract Ameliorates Salt-Induced Aggravation of Nonalcoholic Fatty Liver Disease in Obese Mice Fed a High-Fat Diet. Journal of food science. 2017 Jul;82(7):1765-74.
17. Lin YY, Hsieh PS, Cheng YJ, Cheng SM, Chen CN, Huang CY, Kuo CH, Kao CL, Shyu WC, Lee SD. Anti-apoptotic and pro-survival effects of food restriction on high-fat diet-induced obese hearts. Cardiovascular toxicology. 2017 Apr 1;17(2):163-74.
18. Chiu HW, Chen CH, Chen YJ, Hsu YH. Far-infrared suppresses skin photoaging in ultraviolet B-exposed fibroblasts and hairless mice. PloS one. 2017 Mar 16;12(3):e0174042.
19. Duru N, Zhang Y, Gernapudi R, Wolfson B, Lo PK, Yao Y, Zhou Q. Loss of miR-140 is a key risk factor for radiation-induced lung fibrosis through reprogramming fibroblasts and macrophages. Scientific Reports. 2016 Dec 20;6:39572.
20. Kuo TM, Hsu HT, Chung CM, Yeh KT, Wu CT, Lee CP, Chiang SL, Huang CM, Ko YC. Enhanced alpha-kinase 1 accelerates multiple early nephropathies in streptozotocin-induced hyperglycemic mice. Biochimica et Biophysica Acta (BBA)-Molecular Basis of Disease. 2016 Nov 1;1862(11):2034-42.
21. Zwaans BM, Krueger S, Bartolone SN, Chancellor MB, Marples B, Lamb LE. Modeling of chronic radiation-induced cystitis in mice. Advances in Radiation Oncology. 2016 Aug 1.
22. Chen YF, Shibu MA, Fan MJ, Chen MC, Viswanadha VP, Lin YL, Lai CH, Lin KH, Ho TJ, Kuo WW, Huang CY. Purple rice anthocyanin extract protects cardiac function in STZ-induced diabetes rat hearts by inhibiting cardiac hypertrophy and fibrosis. The Journal of nutritional biochemistry. 2016 May 1;31:98-105.
23. Kwiatkowski A, Piatkowski M, Chen M, Kan L, Meng Q, Fan H, Osman AH, Liu Z, Ledford B, He JQ. Superior angiogenesis facilitates digit regrowth in MRL/MpJ mice compared to C57BL/6 mice. Biochemical and biophysical research communications. 2016 May 13;473(4):907-12.
24. M.-C. Chen, J.-P. Chang, T.-H. Chang, S.-D. Hsu, H.-D. Huang, W.-C. Ho, F.-S. Wang, C.-C. Hsiao, and W.-H. Liu, "Unraveling regulatory mechanisms of atrial remodeling of mitral regurgitation pigs by gene expression profiling analysis: role of type I angiotensin II receptor antagonist," Translational Research, vol. 165, no. 5, pp. 599-620, May 2015.
25. C.-H. Lin, M.-L. Shen, S.-T. Kao, and D. C. Wu, "The effect of sesamin on airway fibrosis in vitro and in vivo," International Immunopharmacology, vol. 22, no. 1, pp. 141-150, Sep. 2014.
26. J.-W. Yu, W.-J. Duan, X.-R. Huang, X.-M. Meng, X.-Q. Yu, and H.-Y. Lan, "MicroRNA-29b inhibits peritoneal fibrosis in a mouse model of peritoneal dialysis," Lab Invest, vol. 94, no. 9, pp. 978-990, Sep. 2014.
27. B.-C. Wu, S.-C. Huang, and S.-J. Ding, "Comparative Osteogenesis of Radiopaque Dicalcium Silicate Cement and White-Colored Mineral Trioxide Aggregate in a Rabbit Femur Model," Materials, vol. 6, no. 12, pp. 5675-5689, Dec. 2013.
28. H. M. Kim, Y. Y. Lim, M. Y. Kim, I. P. Son, D. H. Kim, S. R. Park, S. K. Seo, M. S. Lee, S.-K. Mun, C. W. Kim, and B. J. Kim, "Inhibitory effect of tianeptine on catagen induction in alopecia areata-like lesions induced by ultrasonic wave stress in mice," Clin Exp Dermatol, vol. 38, no. 7, pp. 758-767, Oct. 2013.
29. E. Nusayr, D. T. Sadideen, and T. Doetschman, "FGF2 modulates cardiac remodeling in an isoform- and sex-specific manner," Physiological Reports, vol. 1, no. 4, Sep. 2013.
30. E. Kniazeva, S. Kachgal, and A. J. Putnam, "Effects of Extracellular Matrix Density and Mesenchymal Stem Cells on Neovascularization In Vivo," Tissue Engineering Part A, vol. 17, no. 7-8, pp. 905-914, Apr. 2011.
31. R. Bekeredjian, C. B. Walton, K. A. MacCannell, J. Ecker, F. Kruse, J. T. Outten, D. Sutcliffe, R. D. Gerard, R. K. Bruick, and R. V. Shohet, "Conditional HIF-1α Expression Produces a Reversible Cardiomyopathy,""PLoS ONE, vol. 5, no. 7, p. e11693, Jul. 2010.
32. A.F.I.P. Laboratory Methods in Histotechnology; 1992, pages 132-133.
33. Sheehan, DC., Hrapchak, BB. Theory and Practice of Histotechnology; 1980, page 190.

Diagnostic BioSystems
6616 Owens Drive
Pleasanton, CA, 94588
Tel: (925) 484 3350
www.dbiosys.com

CE IVD

CH REP
MedEnvoy Switzerland
Gotthardstrasse 28
6302 Zug
Switzerland

EC REP
MedEnvoy Global B.V.
Prinses Margrietplantsoen 33 - Suite 123
2595 AM The Hague
The Netherlands